Lipids (2021) **56:** 289–299
DOI 10.1002/lipd.12296

ORIGINAL ARTICLE

Comparison of the Effects of Statins on A549 Nonsmall-Cell Lung Cancer Cell Line Lipids Using Fourier Transform Infrared Spectroscopy: Rosuvastatin Stands Out

Hatice Nurdan Aksoy[1] · **Cagatay Ceylan**[2]

Received: 26 August 2020 / Revised: 27 October 2020 / Accepted: 20 November 2020

Abstract Statins are commonly prescribed antilipidemic and anticholesterol class of drugs. In addition to their major role, they have been found to have anticancer effects on *in vitro*, animal and clinical studies. The aim of this study was to investigate the effects of six different statins (rosuvastatin, pravastatin, simvastatin, lovastatin, fluvastatin, and atorvastatin) on A549 cancer cells lipids by Fourier transform infrared (FTIR) spectroscopy. Proliferation tests were carried out to detect the half-maximal inhibitory concentrations (IC_{50}) of each statin on A549 cells. The IC_{50} values were 50 μM for simvastatin, 150 μM for atorvastatin and pravastatin, and 170 μM for fluvastatin, 200 μM for rosuvastatin and lovastatin on A549 cells. No correlation was found between the antiproliferative effects of the statins and lipid-lowering effect. The cells were treated with IC_5, IC_{10}, and IC_{50} values of each statins concentration and lipid extracts were compared using FTIR spectroscopy. The results indicated that different statins had different effects on the lipid content of A549 cells. The FTIR spectra of the lipid exctracts of statin-treated A549 cells indicated that the value of hydrocarbon chain length, unsaturation index, oxidative stress level, and phospholipid containing lipids increased except for rosuvastatin-treated A549 cells. In addition, rosuvastatin significantly lowered cholesterol ester levels. In conclusion, the contrasting effects of rosuvastatin should be further investigated.

✉ Cagatay Ceylan
cagatayceylan@iyte.edu.tr

[1] Department of Biotechnology, İzmir Institute of Technology, İzmir, 35430, Turkey

[2] Department of Food Engineering, Faculty of Engineering, İzmir Institute of Technology, Urla, 35430, İzmir, Turkey

Published online: 21 February 2021
Lipids (2021) **56:** 289–299

Keywords A549 · FTIR · Lipid · Nonsmall-cell lung cancer · Rosuvastatin · Statin

Lipids (2021) **56:** 289–299.

Abbreviations

ACAT	acyl-cholesterol acyltransferase
ACC	acetyl-CoA carboxylase
ACLY	ATP citrate lyase
DMSO	dimethyl sulfoxide
HMG-CoA	3-hydroxy-3-methyl-glutaryl-Coenzyme A
HMG-CoAR	3-hydroxy-3-methylglutaryl-CoA reductase
FASN	fatty acid synthase
FTIR	Fourier transform infrared
MTT	3-[4,5-dimethylthiazol-2-yl]-2,5-diphenyltetrazolium bromide
NSCLC	nonsmall-cell lung cancer
PtdCho	phosphatidylcholine
PtdEtn	phosphatidylethanolamine
PtdIns	phosphatidylinositol
PtdSer	phosphatidylserine

Introduction

Cancer is a very complicated genetic disease, which is generally characterized by the aberrant mechanisms of cellular differentiation, cell survival, proliferation, and death pathways in a specific tissue. Malignant transformations arise from alterations of oncogenes in the genetic level mutational/recombinational changes in tumor suppressor genes and are well known to result in metabolic reprogramming at the cell level (Evan and Vousden, 2001). Deregulated lipid metabolism was designated as one of the emerging

hallmarks of cancer (Pavlova and Thompson, 2016). One of the altered metabolic changes in tumor cell biology is the aberrant lipid metabolism and cholesterol-associated pathways (Beloribi-Djefaflia et al., 2016). Similarly, altered lipid metabolism can cause carcinogenesis and development of cancer and chemotherapy resistance (Baenke et al., 2013; Zhang and Du, 2012). These alterations include increased expression of several proteins involved in lipid synthesis such as acetyl-CoA carboxylase (ACC), fatty acid synthase (FASN), and ATP citrate lyase (ACLY) in most tumors and the enzymes that promote cholesterol synthesis.

Nonsmall-cell lung cancer (NSCLC) has one of the highest incidence and mortality rates among all types of cancers worldwide (Yu et al., 2013). According to clinical studies, tumorous lung tissues show significant accumulation of total and esterified cholesterol stored in cells. Elevated acyl-cholesterol acyltransferase (ACAT) expression levels and other lipogenic enzymes were reported in hyperplastic and neoplastic growth as well in the lung cancer studies (Dessi et al., 1992).

Cellular cholesterol homeostasis is controlled by *de novo* cholesterol synthesis, cellular influx, and cellular efflux (Goldstein and Brown, 1990). Cholesterol is synthesized at the end of the mevalonate pathway where HMG-CoA is converted to mevalonate by rate-limiting enzyme 3-hydroxy-3-methylglutaryl-CoA reductase (HMG-CoAR). Statins are one class of anticholesterolemic drugs which are called 3-hydroxy-3-methyl-glutaryl-Coenzyme A (HMG-CoA) reductase inhibitors (Tobert, 2003). There are currently six different statins medicated (rosuvastatin, pravastatin, simvastatin, lovastatin, fluvastatin, and atorvastatin). Although all statins have the common dyslipidemic mechanism of action, they have distinct chemical structures, pharmacokinetic profiles, and efficacies. These chemical differences create different water solubility behavior that affects absorption, distribution, metabolism, and excretion for each statin. The antiproliferative effects of statins were also reported on several different cancer types (Jiang et al., 2014). However, none of these studies included a complete characterization of the effects of all statins currently prescribed on cancer cells.

Fourier transform infrared (FTIR) spectroscopy is a rapid, sensitive, and nondestructive vibrational spectroscopic method that monitors the global chemical composition of the sample (Wu et al., 2015). The technique is widely used in many research areas such as biochemistry, biomedicine, biophysics, and biomaterials to investigate structural components of biological samples (Farhadi et al., 2016; Lin et al., 2007). It is used in the analysis of biological systems in any physical state providing molecular fingerprints of tissues and cells (Yandim et al., 2016). It is a valuable analytical technique for detection of metabolic changes in cells, namely proteins, carbohydrates, and nucleic acids, at the level of functional groups on account of the fact that materials have different infrared absorptions and illustrate different vibrations according to their chemical bonds at the suitable wavelength. In addition to the characterization of the chemical nature of cellular molecules, it also accounts for conformational changes to various molecular-functional groups (Derenne et al., 2011). FTIR spectra as well allow to determine changes between normal and cancerous cells and it is used as a diagnostic tool in medicine. The technique qualitatively and quantitatively investigates shifts in peak positions, changes in bandwidths, and band intensities acquiring structural and functional information that offers the opportunity to examine rapid treatment induced during metabolic modifications. This technique can also be used to determine mode of actions of drugs that presents a unique fingerprint of characteristic effects of agents on molecules.

In this study, the antiproliferative, dyslipidemic, and lipid metabolic effects of statins on A549 cancer cells were studied using MTT (3-[4,5-dimethylthiazol-2-yl]-2,5-diphenyltetrazolium bromide) proliferation tests and FTIR spectroscopy.

Materials and Methods

Chemicals

Statins (Lovastatin Hydroxy Acid (sodium salt), Simvastatin (sodium salt), Atorvastatin (calcium salt), Rosuvastatin (calcium salt), Fluvastatin (sodium salt), and Pravastatin (sodium salt)) were purchased from Cayman Chemicals (USA). The stock solutions of each statin were prepared in dimethyl sulfoxide (DMSO) at concentrations of 20 mM, stored at −20 °C and diluted in cell culture medium.

Cell Culture

A549 cells were cultured in high glucose dulbecco's modified eagle medium (DMEM) supplemented with L-glutamine and 10% fetal bovine serum and 1% penicillin–streptomycin in an atmosphere of 5% CO_2 at 37 °C. When the cell confluence reached at 80%, a new cell passage was carried out.

Measurement of Cell Viability by MTT Assay

The antiproliferative effects of statins on A549 cells were determined by MTT cell proliferation assay. MTT (3-[4,5-dimethylthiazol-2-yl]-2,5-diphenyltetrazolium

bromide) is a yellow auxiliary agent that reduced purple formazan crystals in living cells by their active mitochondria (Pearse, 1957; Stockert et al., 2018). 5000 cells were seeded on each well of 96 well plate with growth medium and incubated at 37 °C and in 5% CO_2 for 24–48 h until they gained normal morphology. Then they were treated with different concentrations of each statin. 5 μL of each statin concentration was added to wells for triplicate assay. The last concentration was completed to 100 μL. Following this, the cells were kept at 37 °C in a 5% CO_2 supplemented incubator for 48 h. 10 μL of MTT solution (5 mg/mL in phosphate-buffered saline (PBS)) was added to each well and incubated at 37 °C for 4 h in the carbon dioxide incubator. Then, the plate was centrifuged at 1800 rpm for 10 min and the supernatant phase was removed. 150 μL DMSO was added into each well to dissolve the formazan crystals and kept on shaker at 130 rpm for 10 min. Finally, the absorbance values were measured at 570 nm by a spectrophotometer (Thermo Electron Corporation Multiskan Spectrum, Finland). The number of statin treated living cells and control groups was directly proportional to the intensity of the purple product.

Preparation of Statins

Firstly, 1, 5, 10, 25, 50, 100, 150, 200, 300, and 400 μM dilutions of atorvastatin, fluvastatin, lovastatin, rosuvastatin, simvastatin, and pravastatin were prepared in DMSO from the stock solution for each statin with a concentration of 20 mM. The serial dilutions of each statin were prepared based on this stock solution in DMEM.

Lipid Extraction

For lipid extraction from A549 cells, 3×10^4 cells were seeded into 24 well plates and incubated for 48 h, and the cells were treated with three concentrations determined before MTT at IC_{50}, the fifth of IC_{50} and the tenth of IC_{50} values of each statins. Following the incubation period, the cells were washed with 500 μL PBS then were treated with 100 μL tyrpsin and incubated for 5 min at 37 °C in 5% CO_2. The cells collected by centrifugation in eppendorf tubes at $130 \times g$ for 5 min. After the supernatant phase was removed, the pellets were washed with 500 μL PBS twice. The cell pellets were homogenized with 600 μL of extraction mixture containing chloroform/methanol (2:1, v/v) *via* vortexing. The mixture was incubated for 20 min at the room temperature. Following the incubation period, 180 μL double-distilled water was added into the each of mixture, homogenized with vortexing and centrifuged at $500 \times g$ for 10 min. At the end of the centrifugation, the upper phase was removed by siphoning. 20 μL lipid extract was put on the attenuated total reflectance (ATR-FTIR) diamond. After the solvent was evaporated the spectra was recorded.

FTIR Spectrum Data Analyses

For the lyophilized samples, the spectral analysis was performed by using a Perkin-Elmer spectrometer (USA) equipped with MIR TGS detector (Spectrum 100 Instrument, Perkin Elmer). The FTIR spectra of the samples were recorded between 4000 and 450 cm^{-1} region. The interferograms were recorded with 20 scans at 4 cm^{-1} resolution against the pure potassium bromide as the background. Each sample was studied in triplicate.

For the lipid extracts, the spectral analysis was performed by using a Perkin-Elmer Attenuated total reflectance Fourier transform infrared spectrometer equipped with diamond/ZnSe crystal (UATR Two, Perkin Elmer). FTIR spectra of the samples were recorded between 4000 and 450 cm^{-1} region. The interferograms were recorded with 20 scans at 2 cm^{-1} resolution against the background. Each sample was studied in triplicate. Spectrum 100 (Perkin Elmer) software was used for all of the data manipulations. The triplicates with at least two different scans were performed which gave identical spectra. These replicates were averaged and the averaged spectra for each sample were then used for further data manipulation and statistical analysis. For the visual inspection, the averaged spectra were interactively baselined from three arbitrarily selected points. Finally, the baselined spectra were normalized in specific regions for visual comparison of the samples for the studied parameters and control samples. In the quantitative analysis of the FTIR spectra, the band intensity ratios of certain bands were calculated and reported (Yandim et al., 2016).

Statistical Analysis

The differences between the control and the statin treated cell groups were compared using the Mann–Whitney U Test. The statistical results are expressed as means ± standard deviation. $p < 0.05$ was considered statistically significant.

Results

Antiproliferative Effects of Statins on A549 Cells

To assess the antiproliferative effects of statins on A549, the cells were treated with increasing concentrations of statins (1, 5, 10, 25, 50, 100, 150, 200, 300, and 400 μM)

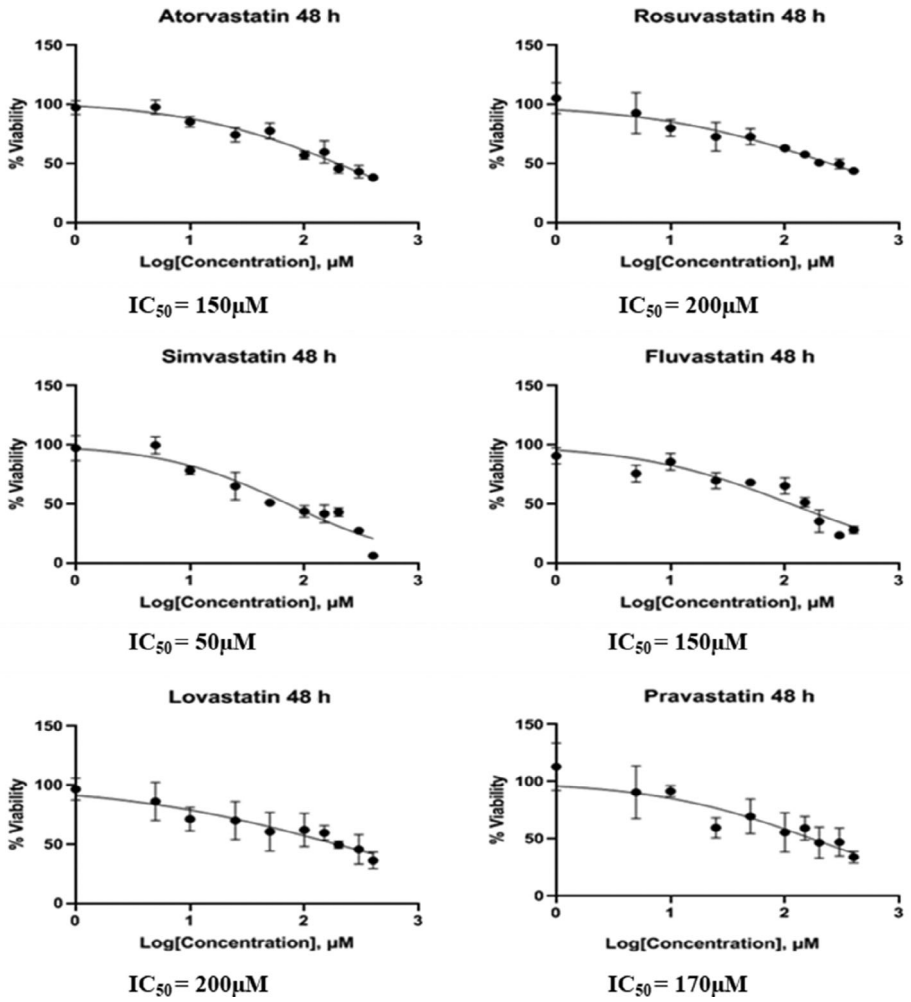

Fig 1 The cytotoxicity profiles of statins on A549 cells

for 48 h and MTT cell proliferation assay was conducted.

The results indicated that A549 cells showed dose-dependent decreasing cell proliferation response as compared to untreated controls. The IC_{50} values for each statins were found as shown in Fig. 1. These values are 150 μM for atorvastatin and pravastatin, 200 μM for rosuvastatin and lovastatin, 50 μM for simvastatin, and 170 μM for fluvastatin.

Statins Cause Lipid Lowering Effects at Varying Amounts

The ratio of the band associated with ester C═O stretching vibration of neutral and phospholipids (1740 cm^{-1}) to the amide I (1600 cm^{-1}) band shows the relative content of cellular lipids and proteins in whole cell extracts (Fabian et al., 1995). As seen in Fig. 2, lovastatin, pravastatin and atorvastatin treatment caused significant decreases in the lipid/protein ratios. In the case of lovastatin increasing the concentration of the statin caused more decreases in the lipid/protein ratio. Simvastatin and fluvastatin caused

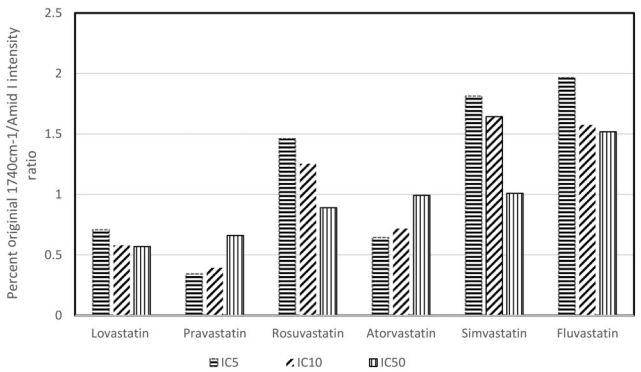

Fig 2 The normalized 1740 cm^{-1}/Amid I ratios of at IC_5, IC_{10} and IC_{50} values for the statin treated A549 cell lyophilizates

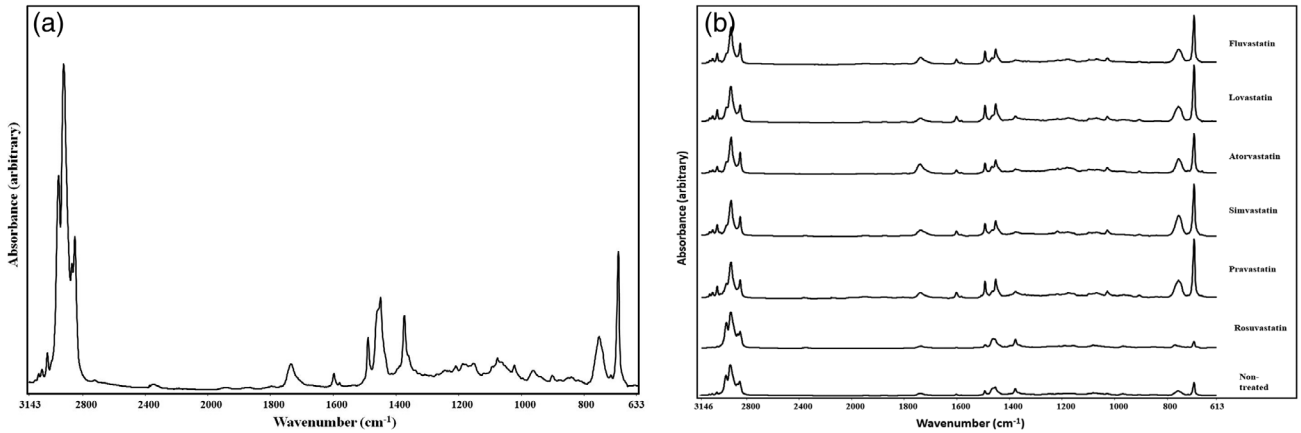

Fig 3 (a) The general Fourier transform infrared (FTIR) spectrum of the lipid extract of A549 cells, (b) comparison of the FTIR spectra of the statin treated A549 cells between 3100 and 680 cm^{-1}

increases in the lipid/protein ratio. The highest lipid/protein ratio was obtained with IC_5 and the lipid lowering effect were even higher for increasing statin concentrations. Rosuvastatin showed a concentration dependent behavior, for example for IC_5 and IC_{10} the lipid/protein ratio was higher than the control A549 cells and lower for the IC_{50} statin concentration.

The FTIR Spectra of Lipid Extracts of Statin-Treated A549 Cells

The effect of statin treatment on the A549 cell lipid metabolism was studied using the control and statin-treated cancer cell lipid extracts. The FTIR spectrum of the lipid extracts of nontreated A549 cells are given in Fig. 3a. The

Table 1 The Fourier transform infrared band assignments of lipid extracts of A549 cells

Wavenumber (cm^{-1})	Assignments	References
3082	C-H ring	(Talari et al., 2017)
3025	Aromatic CH stretching	(Talari et al., 2017)
3001	Olefinic, CH═CH stretching vibration	(Dreissig et al., 2009)
2954	Asymmetric stretching vibration of the CH_3 group	(Galeb et al., 2012)
2922	Asymmetric stretching vibration of the CH_2 group	(Sánchez et al., 2008)
2869	Symmetric stretching vibration of the CH_3 group	(Hayati et al., 2005)
2850	Symmetric stretching vibration of the CH_2 group	(Hayati et al., 2005)
1737	Stretching vibration of the C═O group	(Arrondo and Goni, 1998)
1601	C═C Stretching	(Vidyadharani and Dhandapani, 2013)
1492	Choline, asymmetric bending of the N—CH_3 group	(Schwarzott et al., 2004)
1453	Bending vibrations of the CH_2 groups of fatty acids	(Oleszko et al., 2015)
1377	Bending vibrations of the CH_3 groups of fatty acids	(Dreissig et al., 2009)
1213	Asymmetric stretching vibration PO_2^-	(Yandim et al., 2016)
1157	Stretching vibration of the C—O group of lipid ester bond	(Arrondo and Goni, 1998)
1082	Symmetric stretching vibration of the PO_2^-	(Sánchez et al., 2008)
970	Asymmetric stretching vibration of the C═C group: conformation *trans*	(Yoshida *et al*, 2015)
846	Asymmetric stretching vibration of the P-O	(Dreissig et al., 2009)
698	Stretching vibration of C-C-C ═C-H out-of-plane bending	(Gupta et al., 2014)

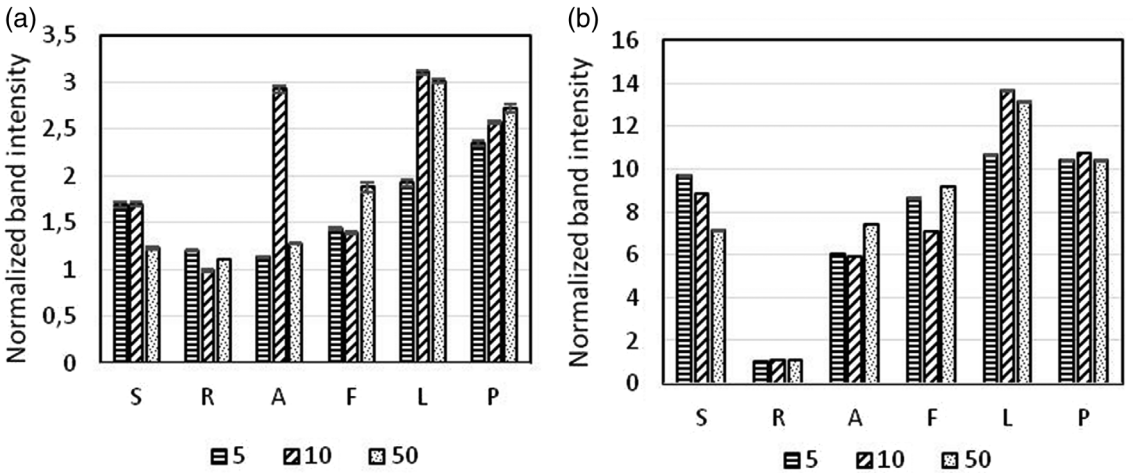

Fig 4 The effect of statin treatments on the intensity in the (a) 3002 cm^{-1} (b) 3082 cm^{-1} band intensities of the statins tested on A549 cells at IC_5, IC_{10} and IC_{50} values. (Simvastatin (S), Rosuvastatin (R), Atorvastatin (A), Fluvastatin (F), Lovastatin (L), Pravastatin (P)). The bands were normalized with respect to the intensity of the bands of control cells

assignments of the major bands in Fig. 3a, b are given in Table 1.

Between 3100 and 2750 cm^{-1} the bands originate from the C—H groups stretching vibrations which are dominated by the fatty acids. The region 1800 between 700 cm^{-1} comprises the fingerprint region; therefore, this region is valuable for classification of lipids (Dreissig et al., 2009). The bands between 3011 and 3000 cm^{-1} originate from unsaturated fatty acids and cholesterol esters (H—C═C—H) and shows unsaturation levels of lipids (Shapaval et al., 2014). The bands at 2954, 2922, 2869, and 2850 cm^{-1} are assigned to asymmetric stretching vibration of the CH_3 and CH_2 group, and symmetric stretching vibration of the CH_3 and CH_2 groups, respectively (Lamba et al., 1991; Oleszko et al., 2015).

The C═O group stretching vibrations at 1737–1740 cm^{-1} originate from fatty esters or cholesterol and triacylglycerol esters and used for the estimation of lipid levels (Yoshida et al., 2009). The band at 1601 cm^{-1}C═C stretch represents the alkene groups (Vidyadharani and Dhandapani, 2013). A band at 1492 cm^{-1} is assigned to choline derived asymmetric bending of the N-CH_3 group (Schwarzott et al., 2004). The bands at 1453 and 1377 cm^{-1} are defined for bending vibrations of the CH_2 and CH_3 groups of fatty acids, respectively. The band between 1213 and 1218 cm^{-1} is

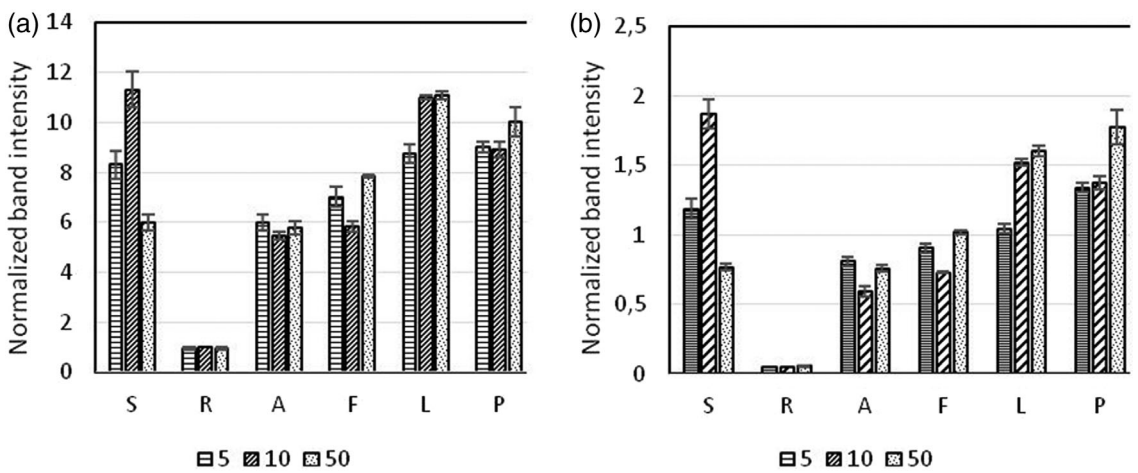

Fig 5 The effect of statin treatments on the band intensities at (a) 697 cm^{-1} and (b) 542 cm^{-1} of A549 cancer cells at IC_5, IC_{10} and IC_{50} values. (Simvastatin (S), Rosuvastatin (R), Atorvastatin (A), Fluvastatin (F), Lovastatin (L), Pravastatin (P)). The bands were normalized with respect to the intensity of the bands of control cells

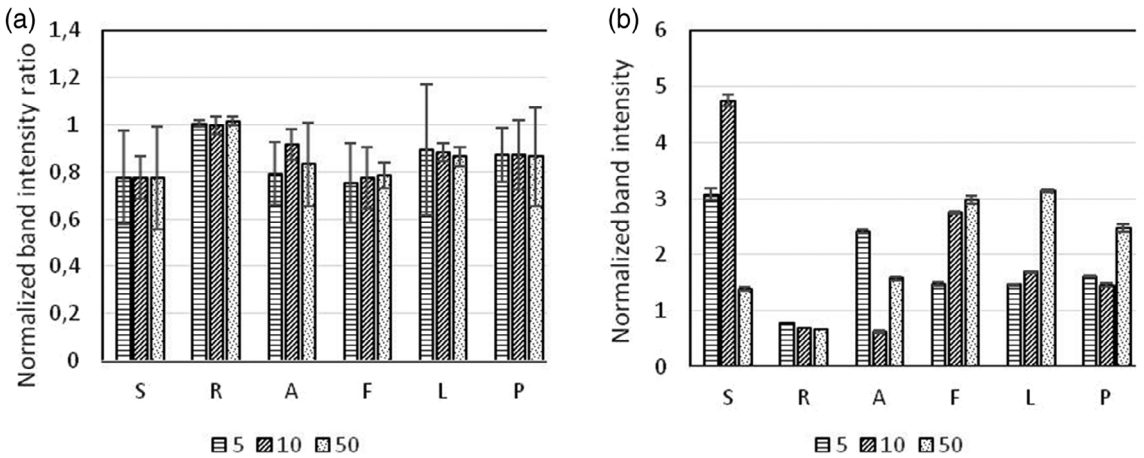

Fig 6 The effect of statin treatments on the band intensity ratio of (a) 2850/2869 cm^{-1} and (b) 1217/2820 cm^{-1} of A549 cancer cells at IC_5, IC_{10} and IC_{50} values. (Simvastatin (S), Rosuvastatin (R), Atorvastatin (A), Fluvastatin (F), Lovastatin (L), Pravastatin (P)). The bands were normalized with respect to the intensity of the bands of control cells

antisymmetric stretching vibration of PO_2^- groups which include phosphatidylinositol (PtdIns), phosphatidylethanolamine (PtdEtn), phosphatidylcholine (PtdCho), and phosphatidylserine (PtdSer), whereas, the band at 1082 cm^{-1} is assigned to symmetric stretching vibration of PO_2^- (Dreissig et al., 2009). The range of the 1157–1179 cm^{-1} is in charge of asymmetric stretching vibration of the C-O group of lipid ester bonds. The band at 1082 cm^{-1} represents the vibration of phospholipids. Vibrations of C-O-P of phospholipids are also observed at 1028 cm^{-1}. A band at 970 cm^{-1} is known as asymmetric vibration of HC═CH (trans-alkene) in fatty acids and represents changes of lipid hydroperoxides with the double bond of trans conjugation (Yoshida et al., 2009). The band at 846 cm^{-1} symbolizes asymmetric vibrations of P-O group and stretching vibration of C-C-C of cholesterol molecules (Dreissig et al., 2009). Finally, the band at 698 cm^{-1} represents cholesterol (Yandim et al., 2016).

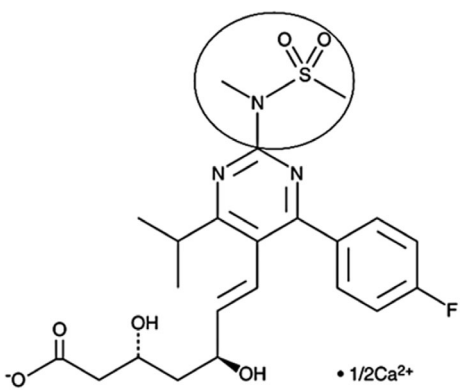

Fig 7 Rosuvastatin molecule (methyl(methylsulfonyl)amino part in circle) (https://www.caymanchem.com/product/12029/rosuvastatin)

Rosuvastatin Decreases Cell Stress and Lipid Unsaturation

The band at 3002 cm^{-1} is an indicator of lipid unsaturation. The absorption at this wavenumber is due to the double bonds between the aliphatic chains of lipids (C═C). Although the band around 3002 cm^{-1} is accepted as an indirect measure of the concentration of lipid peroxidation products, it is better to conceive this band intensity as a measure of unsaturation. The intensity of this band increased for all the statins studied for all of the concentrations studied except for rosuvastatin as shown in Fig. 4a. In general for all the statins tested A549 cells experienced a rapid initial increase in the cellular stress for small concentrations (5% and 10% of the inhibitory concentration) and this increases seem to reach a maximum or steady-state level for higher statin concentrations (50% of the inhibitory concentration).

The bands at 3082, 3060, and 3026 cm^{-1} are representative of aromatic lipids such as eicosanoids and arachidonic acid and its derivatives. When the baselined and normalized spectra were compared between 3100 and 2758 cm^{-1}, the bands around 3080, 3060, and 3026 cm^{-1} were found to have higher intensities when compared with the control spectra for all of the statins except for rosuvastatin. The intensity of these bands showed a marked increase for all of the statins except for rosuvastatin as shown in Fig. 4b for all the statin concentrations studied.

Rosuvastatin Decreases the Cholesterol Content of A549 Cancer Cells as Opposed to the Other Statins

The band at 698 and 542 cm^{-1} are assigned to cholesterol and cholesterol esters, respectively. The intensity of the

band at 698 cm^{-1} decreased slightly with rosuvastatin treatment; however, the treatments with other statins increased the intensity of this band significantly as shown in Fig. 5a. Similarly, the band at 542 cm^{-1} was shown to decrease in intensity with the treatment of rosuvastatin significantly. However, the other statins were shown to cause decrease or increase the amount of cholesterol esters as seen in Fig. 5b.

Rosuvastatin Treatment Reduces the hydrocarbon Chain Length and Phosphate Containing Lipids of A549 Cancer Cells

The hydrocarbon chain length is given by the ratio of the intensities of the CH_2 symmetric stretching band at 2850 cm^{-1} with that of CH_3 symmetric stretching band at 2869 cm^{-1} as seen in Fig. 6a. This ratio was found to be lower than that of the control values for all the statins studied except for the rosuvastatin.

The phosphate containing lipid content is given by the ratio of the PO_2 asymmetric stretching vibration at 1213 cm^{-1} and the CH_2 asymmetric stretching band at 2921 cm^{-1}. This ratio was found to increase when compared with that of their control levels except for rosuvastatin as shown in Fig. 6b.

Discussion

Lung cancer is one of the most prevalent cancer types in the worldwide (Cheng et al., 2016). Abnormal lipid metabolism is an emerging field in the cancer research. Therefore, targeting lipid metabolism in cancer can pave the way for rapid diagnosis and recovery of the disease (Beloribi-Djefaflia et al., 2016). Statins have been frequently used against cardiovascular diseases for the blockage of cholesterol synthesis (Reiner., 2013). Additionally, statins have been found to have antiproliferative properties in many cancer types (Jones et al., 2017; Paškevičiūtė and Petrikaitė, 2017). However, physicochemical properties of statins change according to their chemical structures. Therefore, this study was designed to compare the effects of six commonly used statins on A549 NSCLC cells at the same antiproliferative doses.

The half-maximal inhibitory concentration (IC_{50}) for the most of the statins were already detected on A549 cells by other researchers and in these studies the IC_{50} values of fluvastatin (12 μM), lovastatin (15 μM), and atorvastatin (39 μM) were found to be lower than our results except for simvastatin (Maksimova et al., 2008; Varbanov et al., 2017; Yu et al., 2013). Although there have been considerably lower IC_{50} values reported by other researchers, we proceeded to determine our own values to be able to compare the effects of statins on A549 cells. Therefore, the cytotoxicity values of statins were detected regardless of the literature. The highest antiproliferative effect was found with simvastatin, later atorvastatin and pravastatin, fluvastatin, and finally rosuvastatin and lovastatin.

In this study by using FTIR spectroscopy, the structural differences and cell component changes were determined following the treatment of six different statins at their three different doses.

The band intensity ratio of the 1740 cm^{-1}/Amid I in an FTIR spectrum is generally used for the evaluation of lipid/protein ratio in several biological tissues (Ceylan et al., 2012). Similarly, in this study, this ratio was used to evaluate the effect of statins on the lipid amount with respect to total protein amount since a normalization was carried in this process in the whole cell lyophilizates. The results indicated that the highest dyslipidemic effect was observed with pravastatin, then lovastatin, atorvastatin, rosuvastatin, simvastatin, and fluvastatin in decreasing order. The results indicated that there was no correlation between antiproliferative effect and dyslipidemic effect among the statins. In addition, the dyslipidemic effect was dependent on the concentration of the statin used. Some of the statins showed increasing lipid-lowering effects with increasing statin concentrations (pravastatin and atorvastatin) and the others showed a reverse correlation. Pravastatin, lovastatin, and atorvastatin showed lipid-lowering effects; however, simvastatin, fluvastatin, and rosuvastatin (for the first two concentrations) caused increases in the lipid/protein ratios.

All of the statins used increased the lipid peroxidation with the lowest increase with rosuvastatin as the results of the band intensity at 3001 cm^{-1} was considered. Lipid unsaturation is closely related with membrane dynamics and flexibility. To examine the ratio of unsaturation in lipids, the intensity of the olefinic (HC═CH vibration) band around 3001 cm^{-1} originated from unsaturated fatty acids in the cell was considered (Oleszko et al., 2015; Shapaval et al., 2014). In all of the statin treatments, the unsaturation level showed noticeable increases compared to nontreated A549 cells. However, rosuvastatin and atorvastatin treatment showed small differences. The highest unsaturation level was observed under the lovastatin treatment. Additionally, in accordance with the literature statin treatment caused increasing desaturase activity and lipid unsaturation (Lettiero et al., 2018).

An increasing trend was observed at 757 cm^{-1} for the lipid extracts for all of the statins used. The band around 757 cm^{-1} was reported to originate from linoleic acid (Boyaci et al., 2015). Statins may trigger conversion of linoleic acid to polyunsaturated fatty acids (Risé et al., 2003). Owing to the fact that this band relates to hydroperoxides, peroxidation was found to increase in the statin treated cells (Oyman et al., 2003).

Statins have been known to have dual effects in oxidative stress. In general, they decrease the oxidative stress in organs and tissues and then help heal the body (Liu et al., 2019). Similarly, they were reported to increase the oxidative stress in cancer cells (Sánchez et al., 2008) and to cause cancer cell-specific apoptosis in a number of cancer cell types *via* the inhibition of HMG-CoA reductase (45).

The bands at 3082 cm^{-1} showed significant increases with all of the statins used except for rosuvastatin. Similar to the previous results, rosuvastatin did not cause an increase in the cellular cyclic lipids concentration as a marker of cellular oxidative stress as seen in Fig. 4.

To understand the differences in oxidative stress and lipid unsaturation, we compared the structures of the statin molecules used in the study. All of the statin types had an HMG-CoA analogue region responsible for the inhibition of the HMG-CoA reductase enzyme. Lovastatin, simvastatin, and pravastatin have similar overall structures. Fluvastatin, atorvastatin, and rosuvastatin have a central aromatic ring structure with different attached functional groups. However, rosuvastatin has a methyl(methylsulfonyl)amino group attached to this aromatic centre which is thought to play important functional roles as seen in Fig. 7. This functional group plays an antioxidant function in various biological systems studied (Yan et al., 2020). Statins carry out this antioxidant function by blocking the products of reactive oxygen species and by reducing the NAD+/NADH ratio (Lim and Barter, 2014).

Our results indicated an increase in the saturation status in the rosuvastatin-treated A549 cancer cells. Similar effects of methylsulfonyl containing chemicals were reported to increase the saturation levels of plant systems using the FTIR technique (Prione et al., 2016).

All of the statins used except for rosuvastatin decreased the chain length of the membrane acyl chains. These changes are thought be related to the changes in the elongase enzyme activity levels. Lung cancer cells has high elongase levels (Tang et al., 2018). It is also known that hydrocarbon chain length affects membrane permeability (Uchiyama et al., 2016). Sulfone group containing chemicals were found to inhibit very long chain fatty acid elongases in plants. Although the aforementioned study was carried out in plants, it was important to show that elongase group enzymes were inhibited by sulfone group containing molecules-inhibitors. This inhibitory effect is likely to cause the activity of long chain elongases to decrease. These results are parallel with the results obtained in our study.

To calculate phospholipid-containing lipids content such as phosphatidic acid, glycerophospholipids, phosphatidyl ethanolamine, phosphatidyl choline, phosphatidyl serine, phosphatidyl inpsitole, and glycerophospholipids, the asymmetric stretching band of PO_2 groups at 1217 cm^{-1} was used. When lovastatin, pravastatin, fluvastatin, and simvastatin were applied on the cells, the intensity of this band showed observable increase. The intensity of the band displayed slight decrease for rosuvastatin treatment. Symmetric stretching vibration of PO_2^- groups of phospholipids band at 1082 cm^{-1} significantly increased with the statin treatments, yet only rosuvastatin displayed a slight increase. Sulfone group containing molecules inhibited the long chain elongases. This effect may be responsible for the decrease in the lipid levels which we observed in the phospholipid-containing lipid levels. In addition, the long chain fatty acid elongases take part in the lipidation of some cancer cells (Tamura et al., 2009).

The choline band at 1492 cm^{-1} did not change in rosuvastatin-treated A549 cells. However, the use of other statins caused significant increases in the 1492 cm^{-1} band meaning that statins had significant effects on choline metabolism in connection with phospholipid metabolism except for rosuvastatin.

The intensity of the band at 698 cm^{-1} which is associated with cholesterol increased for all statin treatments for all the doses used except for rosuvastatin as seen in Fig. 5a. However, the esterified form of cholesterol showed significantly low values for rosuvastatin and somewhat lower values for atorvastatin and fluvastatin as seen in Fig. 5b. The same band intensity increased for simvastatin, lovastatin, and pravastatin indicating higher levels of cholesterol esters than that of the control cells. The statin treatments caused elevated amounts of cholesterol found in the structure of cell membranes for the most part. The level of cholesterol esters located in the lipid droplets, varied with the statin type and dose of statin application. These results indicated that the intracellular distribution of cholesterol and cholesterol esters changed with statin use. The increase in the cholesterol levels might be due to high levels of oxidative stress due to the use of elevated levels of statins in cancer cells and contributing to the membrane toughness with less fluidity to prevent the statin transport from extracellular milieu to the cytoplasm. The sensitivity to statins was shown to be heterogeneous in the several cancer types studied (Longo et al., 2019). Similarly, statin resistance seems to be important in determining the cholesterol synthesis related gene response to applied statins.

Conclusion

This study was carried out to investigate the effects of dose-dependent changes of six commonly used statins on A549 cells using FTIR spectroscopy. No correlation was found between the antiproliferative effects of the statins and lipid-lowering effect. Rosuvastatin showed contrasting effects on the cancer cells when compared with the rest of the statins used: lipid peroxidation and oxidative stress increased with

the use of other statins, cholesterol and cholesterol ester levels increased with the use of other statins, hydrocarbon chain length and phosphate containing lipids increased with the use of other statins, with rosuvastatin reverse effects were observed. Rosuvastatin should be investigated in terms of its contrasting effects on cancer cells.

Acknowledgements We thank İzmir Institute of Technology (İYTE) Integrated Research Center-Biotechnology and Bioengineering Central Research Laboratories for providing us the necessary facilities throughout the experiments. This research was supported by The Research Funds of İzmir Institute of Technology (Project no: 2019IYTE0218).

Conflict of Interest The authors declare no conflicts of interest.

References

Arrondo, J., & Goni, F. M. (1998) Infrared studies of protein-induced perturbation of lipids in lipoproteins and membranes. *Chemistry and Physics of Lipids*, **96**:53–68.

Baenke, F., Peck, B., Miess, H., & Schulze, A. (2013) Hooked on fat: The role of lipid synthesis in cancer metabolism and tumour development. *Disease Models & Mechanisms*, **6**:1353–1363.

Beloribi-Djefaflia, S., Vasseur, S., & Guillaumond, F. (2016) Lipid metabolic reprogramming in cancer cells. *Oncogene*, **5**:e189.

Boyaci, I., Temiz, H., Geniş, H., Soykut, E., Yazgan, N., & Güven, B. (2015) Dispersive and FT-Raman spectroscopic methods in food analysis. *RSC Advances*, **5**:56606–56624.

Ceylan, C., Camgoz, A., & Baran, Y. (2012) Macromolecular changes in nilotinib resistant K562 cells; an in vitro study by Fourier transform infrared spectroscopy. *Technology in Cancer Research & Treatment*, **11**:333–344.

Cheng, T., Cramb, S., Baade, P., Youlden, D., Nwogu, C., & Reid, M. (2016) The international epidemiology of lung cancer: Latest trends, disparities, and tumor characteristics. *Journal of Thoracic Oncology*, **11**:1653–1671.

Derenne, A., Gasper, R., & Goormaghtigh, E. (2011) The FTIR spectrum of prostate cancer cells allows the classification of anticancer drugs according to their mode of action. *Analyst*, **136**:1134–1141.

Dessi, S., Batetta, B., Pulisci, D., Spano, O., Cherchi, & R., Lanfrango, G. (1992) Altered pattern of lipid metabolism in patients with lung cancer. *Oncology*, **49**:436–441.

Dreissig, I., Machill, S., Salzer, R., & Krafft, C. (2009) Quantification of brain lipids by FTIR spectroscopy and partial least squares regression. *Spectrochimica Acta Part A: Molecular and Biomolecular Spectroscopy*, **71**:2069–2075.

Evan, G. I., & Vousden, K. H. (2001) Proliferation, cell cycle and apoptosis in cancer. *Nature*, **411**:342–348.

Fabian, H., Jackson, M., Murphy, L., Watson, P., Fichtner, I., & Mantsch, H. (1995) A comparative infrared spectroscopic study of human breast tumors and breast tumor cell xenografts. *Biospectroscopy*, **1**:37–45.

Farhadi, E., Kobarfard, F., & Shirazi, F. H. (2016) FTIR biospectroscopy investigation on cisplatin cytotoxicity in three pairs of sensitive and resistant cell line. *Iranian Journal of Pharmaceutical Research*, **15**:213–220.

Galeb, H., Salimon, J., Eid, E., Nacer, N., Saari, N., & Saadi, S. (2012) The impact of single and double hydrogen bonds on crystallization and melting regimes of Ajwa and Barni lipids. *Food Research International*, **48**:657–666.

Goldstein, J. L., & Brown, M. S. (1990) Regulation of the mevalonate pathway. *Nature*, **343**:425–430.

Gupta, U., Singh, V., Kumar, V., & Khajuria, Y. (2014) Spectroscopic studies of cholesterol: Fourier transform infra-red and vibrational frequency analysis. *Materials Focus*, **3**:211–217.

Hayati, I., Man, Y., Tan, C., & Aini, I. (2005) Monitoring peroxide value in oxidized emulsions by Fourier transform infrared spectroscopy. *European Journal of Lipid Science and Technology*, **107**: 886–895.

Jiang, P., Mukthavaram, R., Chao, Y., Nomura, N., Bharati, I. S., Fogal, V., … Kesari, S. (2014) In vitro and in vivo anticancer effects of mevalonate pathway modulation on human cancer cells. *British Journal of Cancer*, **111.8**:1562–1571.

Jones, H., Fang, Z., Sun, W., Clark, L., Stine, J., Tran, A., … Bae-Jump, V. L. (2017) Atorvastatin exhibits anti-tumorigenic and anti-metastatic effects in ovarian cancer in vitro. *American Journal of Cancer Research*, **7**:2478–2490.

Lamba, O. P., Lal, S., Yappert, M. C., Lou, M. F., & Borchman, D. (1991) Spectroscopic detection of lipid peroxidation products and structural changes in a sphingomyelin model system. *Biochimica et Biophysica Acta (BBA)-Lipids and Lipid Metabolism*, **1081**: 181–187.

Lettiero, B., Inasu, M., Kimbung, S., & Borgquist, S. (2018) Insensitivity to atorvastatin is associated with increased accumulation of intracellular lipid droplets and fatty acid metabolism in breast cancer cells. *Scientific Reports*, **8**:5462.

Lim, S., & Barter, P. (2014) Antioxidant effects of statins in the management of cardiometabolic disorders. *Journal of Atherosclerosis and Thrombosis*, **21**:997–1010. https://www.jstage.jst.go.jp/article/jat/21/10/21_24398/_pdf/-char/en.

Lin, S. Y., Li, M. J., & Cheng, W. T. (2007) FT-IR and Raman vibrational microspectroscopies used for spectral biodiagnosis of human tissues. *Journal of Spectroscopy*, **21**:1–30.

Liu, A., Wu, Q., Guo, J., Ares, I., Rodríguez, J. L., Martínez-Larrañaga, M. R., … Martínez, M. A. (2019) Statins: Adverse reactions, oxidative stress and metabolic interactions. *Pharmacology & therapeutics*, **191**:54–84. https://dx.doi.org/10.1016/j.pharmthera.2018.10.004.

Longo, J., Mullen, P. J., Yu, R., van Leeuwen, J. E., Masoomian, M., Woon, D. T., & Penn, L. Z. (2019) An actionable sterol-regulated feedback loop modulates statin sensitivity in prostate cancer. *Molecular metabolism*, **25**:119–130. https://dx.doi.org/10.1016/j.molmet.2019.04.003.

Maksimova, E., Yie, T., & Rom, W. (2008) In vitro mechanisms of lovastatin on lung cancer cell lines as a potential chemopreventive agent. *Lung*, **186**:45–54. https://dx.doi.org/10.1007/s00408-007-9053-7.

Oleszko, A., Olsztyńska-Janus, S., Walski, T., Grzeszczuk-Kuć, K., Bujok, J., Gałecka, K., … Komorowska, M. (2015) Application of FTIR-ATR spectroscopy to determine the extent of lipid peroxidation in plasma during haemodialysis. *BioMed research international*, **2015**:245607.

Oyman, Z., Ming, W., & Van der Linde, R. (2003) Oxidation of model compound emulsions for alkyd paints under the influence of cobalt drier. *Progress in Organic Coatings*, **48**:80–91.

Paškevičiūtė, M., & Petrikaitė, V. (2017) Differences of statin activity in 2D and 3D pancreatic cancer cell cultures. *Drug Design, Development and Therapy*, **11**:3273–3280.

Pavlova, N. N., & Thompson, C. B. (2016) The emerging hallmarks of cancer metabolism. *Cell Metabolism*, **23**:27–47.

Pearse, A. G. E. (1957) Intracellular localisation of dehydrogenase systems using monotetrazolium salts and metal chelation of their formazans. *The Journal of Histochemistry and Cytochemistry*, **5**: 515–527.

Prione, L. P., Olchanheski, L. R., Tullio, L. D., Santo, B. C., Reche, P. M., Martins, P. F., … Prestes, R. A. (2016) GST activity and

membrane lipid saturation prevents mesotrione-induced cellular damage in Pantoea ananatis. *AMB Express*, **6**:1–12.

Reiner, Ž. (2013) Statins in the primary prevention of cardiovascular disease. *Nature Reviews Cardiology*, **10**:453–464.

Risé, P., Ghezzi, S., & Galli, C. (2003) Relative potencies of statins in reducing cholesterol synthesis and enhancing linoleic acid metabolism. *European Journal of Pharmacology*, **467**:73–75.

Sánchez, C. A., Rodríguez, E., Varela, E., Zapata, E., Páez, A., Massó, F. A., … López-Marure, R. (2008) Statin-induced inhibition of MCF-7 breast cancer cell proliferation is related to cell cycle arrest and apoptotic and necrotic cell death mediated by an enhanced oxidative stress. *Cancer Investigation*, **26**:698–707.

Schwarzott, M., Lasch, P., Baurecht, D., Naumann, D., & Fringeli, U. (2004) Electric field-induced changes in lipids investigated by modulated excitation FTIR spectroscopy. *Biophysical Journal*, **86**: 285–295.

Shapaval, V., Afseth, N. K., Vogt, G., & Kohler, A. (2014) Fourier transform infrared spectroscopy for the prediction of fatty acid profiles in Mucor fungi grown in media with different carbon sources. *Microbial Cell Factories*, **13**:86.

Stockert, J. C., Horobin, R. W., Colombo, L. L., & Blázquez-Castro, A. (2018) Tetrazolium salts and formazan products in cell biology: Viability assessment, fluorescence imaging, and labeling perspectives. *Acta Histochemica*, **120**:159–167.

Talari, A., Martinez, M., Movasaghi, Z., Rehman, S., & Rehman, I. (2017) Advances in Fourier transform infrared (FTIR) spectroscopy of biological tissues. *Applied Spectroscopy Reviews*, **52**:456–506.

Tamura, K., Makino, A., Hullin-Matsuda, F., Kobayashi, T., Furihata, M., Chung, S., … Nakagawa, H. (2009) Novel lipogenic enzyme ELOVL7 is involved in prostate cancer growth through saturated long-chain fatty acid metabolism. *Cancer Research*, **69**: 8133–8140.

Tang, Y., Zhou, J., Hooi, S., Jiang, Y., & Lu, G. (2018) Fatty acid activation in carcinogenesis and cancer development: Essential roles of long chain acyl CoA synthetases. *Oncology Letters*, **16**: 1390–1396.

Tobert, J. A. (2003) Lovastatin and beyond: The history of the HMG-CoA reductase inhibitors. *Nature Reviews Drug Discovery*, **2**: 517–526.

Uchiyama, M., Oguri, M., Mojumdar, E., Gooris, G., & Bouwstra, J. (2016) Free fatty acids chain length distribution affects the permeability of skin lipid model membranes. *Biochimica et Biophysica Acta (BBA) - Biomembranes*, **1858**:2050–2059.

Varbanov, H., Kuttler, F., Banfi, D., Turcatti, G., & Dyson, P. (2017) Repositioning approved drugs for the treatment of problematic cancers using a screening approach. *PLoS One*, **12**:e0171052.

Vidyadharani, G., & Dhandapani, R. (2013) Fourier transform infrared (FTIR) spectroscopy for the analysis of lipid from *Chlorella vulgaris*. *Applied Biology*, **61**:16753–16756.

Wu, B. B., Gong, Y. P., Wu, X. H., Chen, Y. Y., & Chen, F. F., Jin, L. T. (2015) Fourier transform infrared spectroscopy for the distinction of MCF-7 cells treated with different concentrations of 5-fluorouracil. *Journal of Translational Medicine*, **13**:108.

Yan, H. L., Cao, S. C., Hu, Y. D., Zhang, H. F., & Liu, J. B. (2020) Effects of methylsulfonylmethane on growth performance, immunity, antioxidant capacity, and meat quality in Pekin ducks. *Poultry Science*, **99**:1069–1074.

Yandim, M. K., Ceylan, C., Elmas, E., & Baran, Y. (2016) A molecular and biophysical comparison of macromolecular changes in imatinib-sensitive and imatinib-resistant K562 cells exposed to ponatinib. *Tumor Biology*, **37**:2365–2378.

Yoshida, S., Zhang, Q., Sakuyama, S., & Matsushima, S. (2009) Metabolism of fatty acids and lipid hydroperoxides in human body monitoring with Fourier transform infrared spectroscopy. *Lipids in Health and Disease*, **8**:28.

Yu, X., Pan, Y., Ma, H., & Li, W. (2013) Simvastatin inhibits proliferation and induces apoptosis in human lung cancer cells. *Oncology Research Featuring Preclinical and Clinical Cancer Therapeutics*, **20**:351–357.

Zhang, F., & Du, G. (2012) Dysregulated lipid metabolism in cancer. *World Journal of Biological Chemistry*, **3**:167–174.